UC 401
LBL-29238
Preprint

Lawrence Berkeley Laboratory
UNIVERSITY OF CALIFORNIA

Materials & Chemical Sciences Division

Submitted to Marcomolecules

A Monte Carlo Study of Polyelectrolyte Adsorption on a Planar Charged Surface

S. Beltrán, H.H. Hooper, H.W. Blanch, and J.M. Prausnitz

June 1990

For Reference

Not to be taken from this room

LBL-29238
Copy 1
Bldg. 50 Library.

Prepared for the U.S. Department of Energy under Contract Number DE-AC03-76SF00098.

DISCLAIMER

This document was prepared as an account of work sponsored by the United States Government. While this document is believed to contain correct information, neither the United States Government nor any agency thereof, nor the Regents of the University of California, nor any of their employees, makes any warranty, express or implied, or assumes any legal responsibility for the accuracy, completeness, or usefulness of any information, apparatus, product, or process disclosed, or represents that its use would not infringe privately owned rights. Reference herein to any specific commercial product, process, or service by its trade name, trademark, manufacturer, or otherwise, does not necessarily constitute or imply its endorsement, recommendation, or favoring by the United States Government or any agency thereof, or the Regents of the University of California. The views and opinions of authors expressed herein do not necessarily state or reflect those of the United States Government or any agency thereof or the Regents of the University of California.

A MONTE CARLO STUDY OF POLYELECTROLYTE ADSORPTION ON A PLANAR CHARGED SURFACE

Sagrario Beltrán, Herbert H. Hooper, Harvey W. Blanch, and John M. Prausnitz***

Chemical Engineering Department
University of California

and

Materials and Chemical Sciences Division
Lawrence Berkeley Laboratory
1 Cyclotron Road
Berkeley, CA 94720

ABSTRACT

Monte-Carlo simulations are presented for a lattice model of an isolated, partially ionized polyelectrolyte near an impenetrable, oppositely ionized surface. We consider the effects of chain ionization, chain hydrophobicity, surface charge density, and solution ionic strength on the conformational and interfacial properties of the model system. The overall dimensions of model polyelectrolytes in the adsorbed state are found to be similar to those of isolated polyelectrolytes in solution; however, the conformational isotropy characteristic of isolated chains is lost when the polymer adsorbs at an interface. The conformational anisotropy of adsorbed chains is described here by calculating the components of the polymer end-to-end distance in directions parallel and orthogonal to the interface. Detailed structural features of the adsorbed chains are described by the distributions of tails, trains and loops. Tails are found to be favored at low degrees of chain ionization, while trains become more favorable at high degrees of ionization. The number of adsorbed chain segments (e.g., degree of adsorption) increases with the surface charge density, and decreases with increasing solution ionic strength; for some conditions, this degree of adsorption becomes a relatively strong function of external conditions.

This work was supported by the Director, Office of Basic Energy Science, Chemical Sciences Division of the U.S. Department of Energy under Contract Number DE-AC03-76SF 00098.

*Present address: Air Products and Chemicals, Allentown, PA 18195.
** To whom correspondence should be addressed

submitted to: *Macromolecules*, June 1990

I. INTRODUCTION

Polyelectrolytes are important for various technical applications, including use as viscosifiers in oil recovery, flocculants in water treatment, wet-end additives in the papermaking process, and as erosion preventers in soil conditioning. For many applications, the rheological behavior of these systems is of primary interest. However, in other cases, the interactions of polyelectrolytes with surfaces are of major (or primary) concern.

Many experimental and theoretical studies have been reported on the behavior of polyelectrolytes at interfaces. Theories for describing polyelectrolyte adsorption have typically followed (by several years) the development of models for adsorption of uncharged polymers. Hesselink presented in 1972[1,2] the first theory for polyelectrolyte adsorption. Hesselink's model was based on the earlier work of Hoeve[3] (directed at adsorption of *uncharged* flexible polymers); both models require that the segment concentration profile near the surface is known à priori.

Theoretical description of polymer adsorption improved with Roe's[4] development of a multilayer lattice theory in which the segment-density profile near the surface is not specified, but is determined in the calculation. Roe's theory considers only segment-density variations normal to the surface, and does not provide sufficient information to distinguish between different (adsorbed) polymer conformations with identical concentration profiles. Scheutjens et al.[5,6] extended Roe's theory to consider the local conformations of segments at different positions along the polymer backbone by calculating the size and frequency distributions of loops, trains and tails on the chain; Figure 1 gives illustrative definitions of these terms. The existence of tails can strongly affect various properties of adsorbed polymer layers, such as hydrodynamic layer thickness, the stability of colloids in the presence of polymers, and the permeability of porous materials in polymer solutions[7].

The lattice theories of Roe and Scheutjens and Fleer for adsorption of uncharged polymers have been extended to describe adsorption of strong polyelectrolytes[8,9] and adsorption of weak polyelectrolytes[10,11] by including a description of long-range electrostatic interactions. These theories provide some of the most advanced current models for describing polyelectrolyte adsorption; they have been widely applied[12-15]. The main assumption in these theories is that polyion rigidity plays a minor role at the surface, i.e., that the

chain is apparently flexible. This assumption is good for polyelectrolytes at low degrees of ionization, or for solutions of high ionic strength; for other cases, chain stiffness may be important.

Muthukumar[16] used a path-integral approach to derive the defining conditions (i.e., chain-charge density, solution ionic strength, temperature) which induce adsorption of a polyelectrolyte on a charged surface. In that work, the Debye-Hückel approximation was used for the electrostatic surface-polyelectrolyte interaction, limiting the valid range of the theory to low electrostatic potentials (see Section II.A). Unfortunately, no calculations have been presented based on Muthukumar's adsorption criteria; the validity of this theory is not known.

A key question in the study of polyelectrolyte adsorption concerns the structure of the adsorbed polymeric species. Polyelectrolytes in solution (in the absence of a surface) may adopt specific configurations and, under certain conditions, can undergo transitions in which major structural rearrangement occurs[17]. A major question in the adsorption of polyelectrolytes having a specific conformation (in solution) is how much of this conformation is retained upon adsorption.

Questions concerning the interfacial structure of adsorbed polymers, and the (potential) structural changes which occur during adsorption, are difficult to answer completely experimentally. Monte-Carlo simulation can play an important role toward answering these questions by allowing direct observation (for model systems) of specific molecular configurations for polyelectrolytes remote from and near attractive interfaces. We have previously used Monte-Carlo simulation for studying conformations of isolated polyelectrolytes on an infinite lattice (i.e., remote from an interface)[18,19]. In this work, we use Monte-Carlo simulation to examine the conformation of a model polyelectrolyte in the vicinity of a charged surface. We analyze the changes in conformation which the model polyelectrolyte experiences upon adsorption. We describe the conformation of the adsorbed chain by the loops, trains and tails formed at the interface.

II. SIMULATION METHOD

A. Model

Our physical model is a single, flexible polyelectrolyte near an impenetrable, charged interface; Figure 1 shows a two-dimensional representation. We describe here the general features of the model, i.e., when both electrostatic and dispersion-force interactions are possible. In this paper, however, we are concerned with the limiting case with only electrostatic interactions between surface and polyelectrolyte.

The polymer chain in the absence of the surface is identical to the model used in Refs. 18 and 19 for studying configurational properties of isolated polyelectrolytes. The chain is represented as a self-avoiding walk of N segments on a cubic lattice. The distance between lattice sites, l, is taken as 2.52 A. which is the distance between alternate atoms on a carbon-backbone, assuming tetrahedral geometry and a carbon-carbon bondlength of 1.54 A. Thus, the segments here can be considered analogous to the repeat groups on a vinyl polymer (e.g., polyacrylic acid). A fraction λ of the segments carry charge of valence unity; these ionized monomers are equally spaced along the chain. All pairs of non-bonded, nearest neighbor segments interact with potential ε. The solvent is considered to be a continuum.

The configurational energy for the isolated chain is given as a sum of electrostatic and non-electrostatic (dispersion-force) contributions:

$$E = E_{el} + E_{nel} \tag{1}$$

The non-electrostatic energy is

$$E_{nel} = \varepsilon m \tag{2}$$

where m is the total number of contacts between non-bonded, nearest-neighbor segments. The electrostatic energy is the sum over long-range coulombic interactions between all pairs of ionized segments:

$$E_{el} = \sum_{i}^{N-1} \sum_{j=i+1}^{N} u_{ij} \tag{3}$$

Here u_{ij} is described by a screened Debye-Hückel coulombic potential[20]

$$u_{ij} = \frac{z_i z_j e^2}{D r_{ij}} \exp(-\kappa r_{ij}) \tag{4}$$

where $z_i e$ and $z_j e$ are the charges on segments i and j which are separated by distance r_{ij}. The ion valence z is either 1 or 0; when segment i or j is uncharged, $u_{ij}=0$. The dielectric constant D is taken as that of water at 25°C. The inverse Debye screening length, κ, is defined by:

$$\kappa^2 = \frac{4 \pi e^2 N_A \sum_i z_i C_i}{D k T} \tag{5}$$

where N_A is Avogadro's number, C_i is the concentration of ionic species i, k is Boltzmann's constant, and T is the absolute temperature.

In addition we must consider interaction between the polyelectrolyte and the surface. The energy for the polyelectrolyte-surface interaction is a sum of two contributions:

$$E' = E'_{el} + E'_{nel} \tag{6}$$

Since the purpose of this work is to isolate the effect on conformation of electrostatic interactions between the surface and the polyelectrolyte chain, we neglect the non-electrostatic polyelectrolyte-surface interactions. The polymer-surface electrostatic energy, E'_{el}, is the sum of all coulombic interactions between the charged polymer segments and the ionized surface sites:

$$E'_{el} = \sum_{i=1}^{N} u_{si} \tag{8}$$

where u_{si} depends on the charge on segment i and on the electrostatic potential, Φ, at the position of that segment:

$$u_{si} = z_i e \Phi \tag{9}$$

Gouy and Chapman considered the problem of a charged planar surface in contact with an electrolyte solution. They suggested that the ions which neutralize the surface charge are spread into the solution forming a diffuse double layer. We assume that, since the polyelectrolyte solution is very dilute (we are studying a single chain in a medium which is infinite in two dimensions), the polyelectrolyte does not contribute to the ionic strength of the solution. We consider an infinite, uniform surface situated in the y-z plane at $x=0$ and with a homogeneous charge density. The electrostatic potential Φ is a function only of the distance x from the surface; there are no variations of this potential along the y or z coordinates. Thus, we write the Poisson-Boltzmann equation for the variation of the electrostatic potential with distance from the surface in the following form[21]:

$$\frac{d^2\Phi}{dx^2} = \frac{4\pi e}{D}\sum_i z_i n_i \exp\left(\frac{-z_i e \Phi}{kT}\right) \tag{10}$$

where D is the dielectric constant of the medium (water at 25°C), z_i is either a positive or negative valence number for the ions in solution, and n_i is the concentration of ions of type i in solution.

Equation (10) can be solved by considering only the situation in which $z_i e\Phi<kT$, so that the exponential can be expanded as a power series. Eqn. (10) then takes a simple form with an explicit solution. Evaluating the potential at 25°C for a monovalent ion which satisfies the condition $z_i e\Phi=kT$, a potential of 25.7 mV is obtained. Thus, potentials may be regarded as low or high, compared to a potential of (about) 25 mV. Debye and Hückel[21] made the assumption of low potentials in their theory known as the Debye-Hückel approximation.

Gouy and Chapman solved the Poisson-Boltzman equation without the low potential assumption for a symmetrical electrolyte solution ($z_i=z$ *and* $n_i=n$ for all the ions in solution) to obtain the variation of the electrostatic potential with distance from the charged surface. By introducing the substitution:

$$b = 2kT/ze \tag{11}$$

the expression obtained for the potential is[21]:

$$\Phi = b \ln \frac{\exp\left(\frac{\Phi_o}{b}\right) + 1 + \left[\exp\left(\frac{\Phi_o}{b}\right) - 1\right] e^{-\kappa x}}{\exp\left(\frac{\Phi_o}{b}\right) + 1 - \left[\exp\left(\frac{\Phi_o}{b}\right) - 1\right] e^{-\kappa x}} \tag{12}$$

where κ is the inverse Debye screening length as defined in equation (5), x is the coordinate normal to the surface and Φ_o is the potential at $x=0$; that potential is a function of the surface charge density σ[21]:

$$\Phi_o = b \sinh^{-1}\left[\sigma\left(2 \frac{D}{\pi} \kappa T n\right)^{1/2}\right] \tag{13}$$

Initially, both the Debye-Hückel[21] and Gouy-Chapman[20] theories were used for calculating the potential Φ, and results of the two methods were compared. For surface potentials below approximately 40 mV, the two theories give essentially the same results; however, for higher potentials, significant differences between the two methods were observed. Thus, all calculations reported here were made using Gouy-Chapman theory.

The total configurational energy of the polyelectrolyte-interface system, E_{tot}, is the sum of the electrostatic polyelectrolyte-surface energy and both electrostatic and non-electrostatic energies for the segment-segment interactions.

$$E_{tot} = E + E'_{el} \tag{14}$$

where E is obtained from Eqn. (1), and E'_{el} from Eqn. (8).

B. Sampling Method

We consider in this work several features of polyelectrolyte adsorption. First, for a polyelectrolyte which can "see" a charged interface, we wish to know how close that polyelectrolyte may migrate to the interface (i.e., whether or not it adsorbs, and how strongly it does so). Second, for cases where adsorption occurs, we are interested in the interfacial structure of the adsorbed species as described by the local conformation at the surface (see Section C below). Finally, we want to examine how the adsorption process affects overall chain dimensions

and structure with respect to the dilute chain remote from an interface. Thus, we need to efficiently sample the configurational space of the polyelectrolyte itself (i.e., the internal chain structure), and the configurational space of the overall system (i.e., allowing the polyelectrolyte to migrate close to, or remain remote from the surface). We describe below the sampling procedure employed here.

The chain was initially placed in a three-dimensional staircase configuration, and then allowed to undergo elementary motions. As in Ref. 19, two general types of chain movements were used: reptation and "internal" motions. Reptation[22] motions resemble a 'slithering' of the chain along the lattice resulting in a net forward or backward displacement of all segments; these motions allow the polyelectrolyte to efficiently explore its environment, i.e., either to migrate to or remain remote from the interface. Internal motions involve the rearrangement of one or two internal-chain segments, and allow for efficient sampling of high-density conformations (e.g., collapsed or adsorbed conformations). As in Ref. (19), we use here both reptation and internal motions for sampling; the two types of movements are attempted with equal frequency.

Successive 'trial' configurations (generated from elementary chain motions) are accepted based on the probability

$$p_{s+1} = \min\{1, \exp(-\Delta E/kT)\} \tag{15}$$

where ΔE is the energy change in going from configuration s to trial configuration $s+1$. When a trial move is accepted, configuration $s+1$ becomes configuration s, and a new move is attempted (i.e., a new trial configuration $s+1$ is generated). When a trial move is rejected, the old configuration (s) is retained and considered as the new state. In this manner, the polymer *evolves* through a sequence (or chain) of configurations generated by successive cycles (attempted elementary motions).

After relaxing the initial configuration through 5×10^4 cycles, the system was allowed to evolve through 2×10^6 cycles, and chain properties were calculated and recorded every 10^4 cycles. The specific initial conformation used is unimportant since its memory is lost during the relaxation step. All simulations were performed with 40-segment chains; the sampling frequency

10^4 cycles was found satisfactory for producing essentially uncorrelated configurations for this chain length.

C. Calculated properties

We describe here the properties used for characterizing chain configuration and position relative to the surface. These properties were calculated every 10^4 cycles during a simulation, and ensemble averages of these properties (denoted by < >) were calculated at the end of a simulation run.

Due to the anisotropic shape of an adsorbed polymer, the three components of the end-to-end distance are not equal. Mean-square end-to-end distance $<r^2>$, as well as the components of this distance orthogonal ($<r^2>_o$) and parallel to the surface ($<r^2>_p$) were calculated as:

$$<r^2> = <(r_n - r_1)^2> \tag{16}$$

$$<r^2>_o = <(x_n - x_1)^2> \tag{17}$$

$$<r^2>_p = <(y_n - y_1)^2 + (z_n - z_1)^2> \tag{18}$$

Similarly, it is useful to compute the contributions to the mean-square radius-of-gyration $<s^2>$ in the planes parallel $<s^2>_p$ and orthogonal $<s^2>_o$ to the surface.:

$$<s^2> = \frac{1}{N} <\sum_{i=1}^{N} (r_i - r_{cm})^2> \tag{19}$$

$$<s^2>_o = \frac{1}{N} <\sum_{i=1}^{N} (x_i - x_{cm})^2> \tag{20}$$

$$<s^2>_p = \frac{1}{N} <\sum_{i=1}^{N} (y_i - y_{cm})^2 + (z_i - z_{cm})^2> \tag{21}$$

Here x_i, y_i, and z_i are the Cartesian coordinates of bead i; r_i is the position vector locating the ith bead, and subscript cm stands for the center of mass of the chain. The end-to-end distances and radii of gyration are reported in this work as reduced variables. The mean-square end-to-end distance and its components

are reduced by the value they would have in a fully extended configuration, $(N-1)^2 l^2$, and the mean-square radius of gyration and its components are reduced by $(N-1)l^2$.

The surface is located in the y-z plane (orthogonal to the x axes) at $x=0$. Lattice layers are numbered $ly=1,\ldots,100$. The surface layer is at lattice layer $ly=0$. To determine the position of the chain relative to the surface, we calculate the average distance from the surface of the chain center of mass, and the segment-density distribution along the coordinate normal to the surface.

To characterize the conformation of the adsorbed polyelectrolyte chain, we consider the content of local conformations known as tails, trains, and loops. Figure 1 shows (in two dimensions) two potential conformations for a 20-segment chain. Trains are consecutive segments in contact with the surface; loops are consecutive segments between trains, and tails are series of segments at the chain ends which are not in contact with the surface. The number of segments in a loop, train, or tail determines its size; i.e., the chain in Figure 1a consists of 2 tails of sizes 4 and 2, 2 trains of size 3, 1 train of size 2, and two loops of sizes 4 and 2. Figure 1b shows a configuration where the ends of the chain are trains of respective sizes 4 and 1; this configuration does not contain tails.

We use here two different types of distributions to present information concerning loop, train, and tail content in adsorbed chains. In the first type of distribution, we are concerned with how far into the solution (i.e., away from the surface) the different types of elementary structures protrude. Thus, for a given lattice layer parallel to the surface, we count the number of segments in that layer contributing to each of the three structures of interest. Trains are always in layer $ly=1$, and thus are not considered in this distribution. For this first distribution, we plot the number frequency of segments contributing to the three types of structures as a function of lattice layer away from the surface (i.e., distance into solution). The second type of distribution is concerned with the *size* frequency of the three types of local structures. Here, we plot the relative frequencies of loops, trains, and tails as a function of structure size. The differences between the two distributions is seen more readily in the discussion of results that follows.

III. RESULTS AND DISCUSSION

We consider here the effects of polymer, solution, and surface conditions on the structural and adsorption properties of our model system. In references 18 and 19 we investigated the configurational properties of *isolated* polyelectrolytes (i.e., in the absence of an interface); ref. 18 considered *hydrophilic* polyelectrolytes (segment-segment potential $\varepsilon/kT=0$), and ref. 19 considered hydrophobic polyelectrolytes ($\varepsilon/kT<0$). Hydrophilic polyelectrolytes experience only repulsive intrachain interactions (i.e., excluded-volume and electrostatic interactions); thus, these chains are always expanded relative to the unperturbed state. Hydrophobic polyelectrolytes experience (effective) attractive segment-segment interactions which compete with excluded-volume and coulombic repulsions; under certain conditions, these hydrophobic polyelectrolytes undergo dramatic structural transitions from an expanded to a collapsed configuration in response to increasing chain ionization.

In this work we isolate the effects of electrostatic segment-surface interactions on system behavior. We thus set the segment-surface non-electrostatic energy to zero. From Ref. 18 we know that dramatic structural transitions are *not* seen for isolated hydrophilic polyelectrolytes; however, hydrophilic chains do exhibit a rich variety of configurational properties, varying from random coil to (near) rigid-rod conformation, depending on the relative magnitudes of system length scales. Using the results of Refs. 18 and 19 as a basis, we investigate here the effect of polymer-surface electrostatic interactions on chain conformation for a hydrophilic and a hydrophobic polyelectrolyte.

We investigate system behavior as a function of chain ionization (λ), Debye screening length (κ^{-1}), and surface charge density (σ). All runs were performed for 40-segment chains, and chain ionization varied from $\lambda=0$ (no charged beads) to $\lambda=0.5$ (20 charged beads). Four values of κ^{-1} were used corresponding to 1:1 electrolyte concentrations of 1.0M ($\kappa^{-1}=3.04$ A), 0.1M ($\kappa^{-1}=9.62$ A), 0.01M ($\kappa^{-1}=30.4$ A), and 0.001M ($\kappa^{-1}=96.2$ A); the surface-charge density varied between 0.0005 and 0.05 e/A^2.

Figures 2 present the effect of surface-charge density (σ) and polyelectrolyte ionization (λ) on the orthogonal, parallel and total components of the end-to-end distance for the case where there are no segment-segment non-electrostatic interactions ($\varepsilon/kT=0$) and the ionic strength ($0.001M$) is low

enough not to screen the electrostatic effects. In Ref. 18 it was found that polyions exhibit a transformation from flexible-chain to rigid-rod behavior as the degree of chain ionization increases. Figures 2 show that polyelectrolytes near a charged surface experience the same transformation in chain dimensions with increasing ionization. Figure 2a shows that the parallel component of the end-to-end distance depends little on the surface charge density. The orthogonal component of the chain end-to-end distance depends more noticeably on the surface-charge density, but only for high polyelectrolyte ionization. The total end-to-end distance (see Figure 2b) does not change significantly compared with that for the isolated polyelectrolyte in solution (Ref. 18).

Figure 3 presents the dependence of the mean-square radius of gyration on surface charge density and degree of ionization; the results in Figure 3 are analogous to those seen in Figure 2 for the end-to-end distance.

From Figures 2 and 3 we observe that the overall dimensions and flexibility (or stiffness) of the adsorbed polyelectrolytes are very similar to those of isolated polyelectrolytes in solution at the same conditions. The primary difference in configurational properties between the isolated and adsorbed polyelectrolytes appears to be in the loss of conformational isotropy for the adsorbed case (i.e., the contribution of the different components in space to the configurational properties are not the same when the polyelectrolyte is adsorbed). As the polyelectrolyte adsorbs, its conformation flattens to decrease the orthogonal components of the end-to-end distance and radius-of-gyration.

Figure 4 shows the effect of surface-charge density (σ) and polyelectrolyte ionization (λ) on the orthogonal and parallel components of the mean-square end-to-end distance when polymer segments interact with a pair potential $\varepsilon/kT=-1$. Again, the ionic strength is chosen to be sufficiently low (0.001M) such that electrostatic effects are not highly screened. We plot the parallel and orthogonal components of the end-to-end distance vs degree of ionization to allow comparison of our results with those of Ref. 19 for isolated hydrophobic polyelectrolytes. In Ref. 19 large transitions in polymer dimensions were observed in response to small changes in chain ionization. Figure 4b shows that, as ionization increases, the overall end-to-end distance of polyelectrolytes near an attractive interface undergoes a transition similar to that seen in Ref 19 for isolated polyelectrolytes. However, Figure 4a shows that this transition in chain dimensions is strongly anisotropic; the transition occurs primarily in the

parallel component of the end-to-end distance, while the orthogonal component gradually *decreases* with increasing ionization.

Figures 2-4 consider chain behavior in solution with a constant ionic strength of 0.001M. Figures 5 and 6 consider the effect of ionic strength on chain end-to-end distance. Here the surface-charge density is fixed at $\sigma=0.005$ e/A^2, and non-electrostatic interactions between polymer segments are set to zero (i.e., $\varepsilon/kT=0$). As ionic strength rises, electrostatic interactions (both chain-surface and segment-segment) are screened and their effects weaken. As the electrostatic surface-segment interactions (which work to flatten the chain on the surface) are reduced with rising ionic strength, the orthogonal component of the end-to-end distance also *rises* (Figure 5a). However, the overall chain end-to-end distance *falls* with rising ionic strength (as in the isolated chain case of Ref. 18) because of the screening of *intrachain* electrostatic repulsions (Figure 5b). When the ionic strength is 1M, the chain is essentially desorbed (see Figure 6) and the contributions of the three components to the end-to-end distance converge to the same value; at this point the parallel component is approximately twice that of the orthogonal component. The influence of ionic strength on chain dimensions becomes less noticeable for low degrees of ionization.

Summarizing the results of Figure 5, we see that the influence of ionic strength on the *overall* chain dimensions (Figure 5b) of an adsorbed polyelectrolyte is very similar to that for an isolated polyelectrolyte[18]. However, an analysis of the separate end-to-end distance components (Figure 5a) shows a pronounced anisotropic variation which indicates a transformation in chain *shape*. This change in shape accompanies chain desorption.

Figure 6 shows clearly the chain desorption induced when the ionic strength rises. Figure 6 is a representation of the variation in the number of adsorbed segments (expressed as a percentage of total segments) with increasing ionic strength for different degrees of ionization. At low ionic strength (0.001M), the percent of segments which are adsorbed increases from 0 to nearly 90% as chain ionization increases from 0 to 0.5. As ionic strength rises, the number of adsorbed segments falls, until at 1.0M the chain does not adsorb to the surface for any of the degrees of ionization studied. Comparing Figures 5 and 6, we see that the larger the number of adsorbed segments in the chain, the more planar its configuration; (i.e. as adsorption increases, the contribution of the orthogonal component to the total end-to-end distance decreases). When the

chain is not adsorbed (e.g., ionic strength of 1M), the contributions of the three components to the end-to-end distance are approximately the same (see Figure 5a).

Figure 7 shows the variation in the number of adsorbed segments as a function of surface-charge density for different degrees of chain ionization. As the surface-charge density increases, the number of segments adsorbed to the the ionized surface increases. This effect is stronger for higher degrees of chain ionization.

Figure 8 considers the effect of *degree of adsorption* (i.e., how tight and close a chain is held to a surface) on the detailed interfacial features of the polymer chains. Figures 8a and 8b present distributions of segment densities, along with loop, train and tail content, for chains which are qualitatively analogous to those shown in the corresponding column of Figure 8c. Figures 8a show the segment-density distribution along the coordinate perpendicular to the surface, and the density distribution of segments that are part of a loop or a tail for the following conditions: surface charge density $\sigma=0.005\ e/A^2$, ionic strength $I.S.=0.001M$ and pair potential interaction between polymer segments $\varepsilon/kT=0$. Figures 8b show the distribution of tails, trains and loops by size for the same conditions. The degree of chain ionization varies; $\lambda=0.1$ in Figures 8(a-b).1; $\lambda=0.2$ in Figures 8(a-b).2 and $\lambda=0.5$ in Figures 8(a-b).3.

The three graphs in Figures 8a, show that the segment-density distribution narrows as the degree of ionization, λ, increases and the chain adsorbs more strongly. For $\lambda=0.5$, the chain remains primarily in the three lattice layers closest to the surface, and nearly 90% of the segments are adsorbed; the number of adsorbed segments (segments in lattice layer $ly=1$) increases with the degree of ionization. Figure 8a.1 shows that for $\lambda=0.1$, the segment-density distribution is mostly composed of tails, and these tails extend as far as 15 lattice layers away from the surface; loops are a relatively minor contribution in this case. The contribution of tails to the total segment density distribution decreases as the degree of ionization increases, and as the number of segments forming trains undergoes a corresponding increase. Thus, we see that for low degrees of chain ionization, tails extend further from the surface than loops, and these tails comprise the main contribution to the thickness of the adsorbed layer. However, as chain ionization rises (and adsorption increases), the contributions of tails and loops to the adsorption layer become approximately equal.

Figures 8b show that for a degree of ionization of $\lambda=0.1$ (Fig. 8b.1) there is a large number of 40-segment tails. Since we are studying a 40-segment chain, a 40-segment tail indicates that none of the segments of the chain are adsorbed (free chain). However, we saw in Figures 8a.1 that the chain is attracted to the surface at these conditions. Long tails are favored at low degrees of ionization, while short tails become more favorable as the degree of ionization (and adsorption) increases; for $\lambda=0.5$, long tails are rare. The segment which ends a tail (i.e., the first adsorbed segment starting from either end of the chain) is more likely to be an ionized segment than one that is uncharged. This is seen in Figures 8b by small maxima for such tail sizes; i.e., in Fig. 8b.1 the distribution for a 10% ionized chain (where the charged segments are positioned in segments number 5, 15, 25, and 35) has maxima for tails which are 4, 14, 24, and 34 segments long respectively. Trains are scarce and short for a 10% ionized chain. As the chain degree of ionization increases, the number of small trains initially rises, and then falls while the number of long trains increases.

Figures 8 consider the case of a hydrophilic polyelectrolyte. For a hydrophobic polyelectrolyte, the distributions of segments, tails, trains and loops show a large number of small trains and loops when the chain ionization is low so that the chain is collapsed, and loops and tails do not protrude as far into the solution as for the hydrophilic polyelectrolyte. When the degree of chain ionization is high enough to adopt a more stretched configuration, all the distributions are similar to those for the hydrophilic polyelectrolyte.

IV. CONCLUSIONS

We have studied the behavior of an isolated, partially ionized polyelectrolyte near an impenetrable, oppositely charged surface using Monte-Carlo simulation. Configurational properties for the polyelectrolyte near the attractive interface were compared with those for an isolated polyelectrolyte. Differences for the overall end-to-end distance and radius of gyration between the two cases were small. However, large anisotropy was seen between the various components of the chain dimensions when the polyelectrolyte is close to (or adsorbed on) the surface.

The solution ionic strength affects both chain configurational properties and the tendency of the chain to adsorb. At low ionic strength, charge

screening is negligible and electrostatic attractions between the surface and chain cause the polyelectrolyte to flatten out and adsorb on the surface. As ionic strength increases, both surface-chain attractions and segment-segment repulsions are screened; thus, the chain assumes a flexible-coil configuration and does not adsorb to the surface.

The detailed interfacial properties of adsorbed chains were studied by considering the distributions of elemental structures such as tails, trains and loops. At low degrees of chain ionization, long tails are favored and the chain is adsorbed to the surface by a small number of segments. At high degrees of ionization, long trains are favored, thereby increasing the number of segments adsorbed to the surface. The number of adsorbed chain segments also increases with rising surface charge-density, and decreases with rising ionic strength of the solution.

ACKNOWLEDGEMENTS

This work was supported by the Director, Office of Energy Research, Office of Basic Energy Sciences, Chemical Sciences Division of the U.S. Department of Energy under contract No. DE-AC03-76SF00098. S.B. is grateful to the Spanish Ministry of Education and Science (MEC) for a fellowship. The calculations reported here were performed on the IBM 3090 at the U.C. Berkeley Computing Center; we acknowledge with thanks the generous computation time provided by the Computing Center. The authors are grateful to Kevin Mansfield and Doros Theodorou for helpful comments.

REFERENCES

1. Hesselink, F. Th. *J. Electroanal. Chem. Interfacial Electrochem.* **1972**, 37, 317.
2. Hesselink, F. Th. *J. Colloid Interface Sci.* **1977**, 60, 448.
3. Hoeve, C. A. J. *J. Polym. Sci.(C)* **1971**, 34, 1.
4. Roe, R. J. *J. Chem. Phys.* **1974**, 60, 4192.
5. Scheutjens, J. M. H. M.; Fleer, G. J. *J. Phys. Chem.* **1979**, 83, 1619.
6. Scheutjens, J. M. H. M.; Fleer, G. J. *J. Phys. Chem.* **1980**, 84, 178.
7. Scheutjens, J. M. H. M.; Fleer, G. J.; Cohen Stuart M. A. *Colloids and Surfaces* **1986**, 21, 285.
8. Van der Schee, H. A.; Lyklema, J. *J. Phys. Chem.* **1984**, 88, 6661.
9. Papenhuijzen, J.; Van der Schee, H. A.; Fleer, G. J. *J. Colloid Interface Sci.* **1985**, 104, 540.
10. Evers, O. A.; Fleer, G. J.; Scheutjens, J. M. H. M.; Lyklema, J. *J. Colloid Interface Sci.* **1986**, 111, 446.
11. Böhmer, M. R.; Evers, O. A.; Scheutjens, J. M. H. M. *Macromolecules* **1990**, 23 2288.
12. Marra, J.; Van der Schee, H. A.; Fleer, G. J.; Lyklema, J. *Adsorption from Solution.* (Ottewill, R. H.; Rochester, C. H.; Smith, A. L., Eds.). Academic Press, New York/London, 1983. p 245.
13. Papenhuijzen, J.; Fleer, G. J.; Bijterbosch, B. H. *J. Colloid Interface Sci.* **1985**, 104, 553.
14. Cohen Stuart M. A. *J. Phys.France* **1988**, 49, 1001.
15. Blaakmeer, J.; Böhmer, M. R.; Cohen Stuart M. A.; Fleer, G. J. *Macromolecules* **1990**, 23 2301.
16. Muthukumar, M. *J. Chem. Phys.* **1987**, 86, 7230.
17. Oosawa, F. *Polyelectrolytes*, Marcel Dekker Inc New York, 1971.
18. Hooper, H. H.; Blanch, H. W.; Prausnitz, J. M. *Macromolecules*, **1990**, in press.
19. Hooper, H. H.; Beltran, S.; Sassi, A. P.; Blanch, H. W.; Prausnitz, J. M. *J. Chem. Phys.* **1990**, in press.
20. Rieger P.H. *Electrochemistry;* Prentice Hall, Inc., 1987; Chapter 2.
21. Hiemenz P.C. *Principles of Colloid Surface Chemistry*, 2nd ed.; Marcel Dekker, Inc., 1986; Chapter 12.
22. Wall, F. T.; Mandel, F. *J. Chem. Phys.* **1975**, 63 4592.

List of Figure Captions

Figure 1. Schematic representation of two potential conformations for a 20-segment adsorbed chain in two dimensions. The chain is represented as a sequence of tails, trains and loops when adsorbed to a planar surface.

Figure 2. Effect of surface-charge density and degree of ionization on polyelectrolyte mean-square end-to-end distance for $\varepsilon/kT=0$ and ionic strength$=0.001M$: (a) parallel (—) and orthogonal (----) components; (b) overall (3-dimensional) mean-square end-to-end distance.

Figure 3. Effect of surface-charge density and degree of ionization on polyelectrolyte mean-square radius of gyration for $\varepsilon/kT=0$ and ionic strength$=0.001M$: (a) parallel (—) and orthogonal (----) components; (b) overall (3-dimensional) mean-square radius-of-gyration.

Figure 4. Effect of degree of ionization and surface-charge density on polyelectrolyte mean-square end-to-end distance for $\varepsilon/kT=-1$ and ionic strength$=0.001M$: (a) parallel (—) and orthogonal (----) components; (b) overall (3-dimensional) mean-square end-to-end distance.

Figure 5. Effect of ionic strength and degree of ionization on polyelectrolyte mean-square end-to-end distance for $\varepsilon/kT=0$ and $\sigma=0.005$ e/A^2: (a) parallel (—) and orthogonal (----) components; (b) overall (3-dimensional) mean-square end-to-end distance.

Figure 6. Effect of ionic strength on the percentage of segments adsorbed to the surface for different degrees of chain ionization. Here, the surface charge density $\sigma=0.005$ e/A^2, and the segment-segment non-electrostatic potential $\varepsilon/kT=0$.

Figure 7. Effect of surface charge density on the percentage of segments adsorbed to the surface for different degrees of chain ionization. Here, ionic strength$=0.001M$ and $\varepsilon/kT=0$.

Figure 8. Interfacial polyelectrolyte conformations and structure for $\sigma=0.005$ e/A^2, ionic strength$=0.001M$, and $\varepsilon/kT=0$: (a) Segment-density distribution (—), density distribution of segments contained in loops (·–·–·), and density distribution of segments contained in tails (----) along the coordinate orthogonal to the surface; (b) Size-frequency distribution of tails (----), trains (—),and loops (·–·–·); (c) Schematic illustrations of the different conformations adopted by an adsorbed chain as a function of degree of ionization.

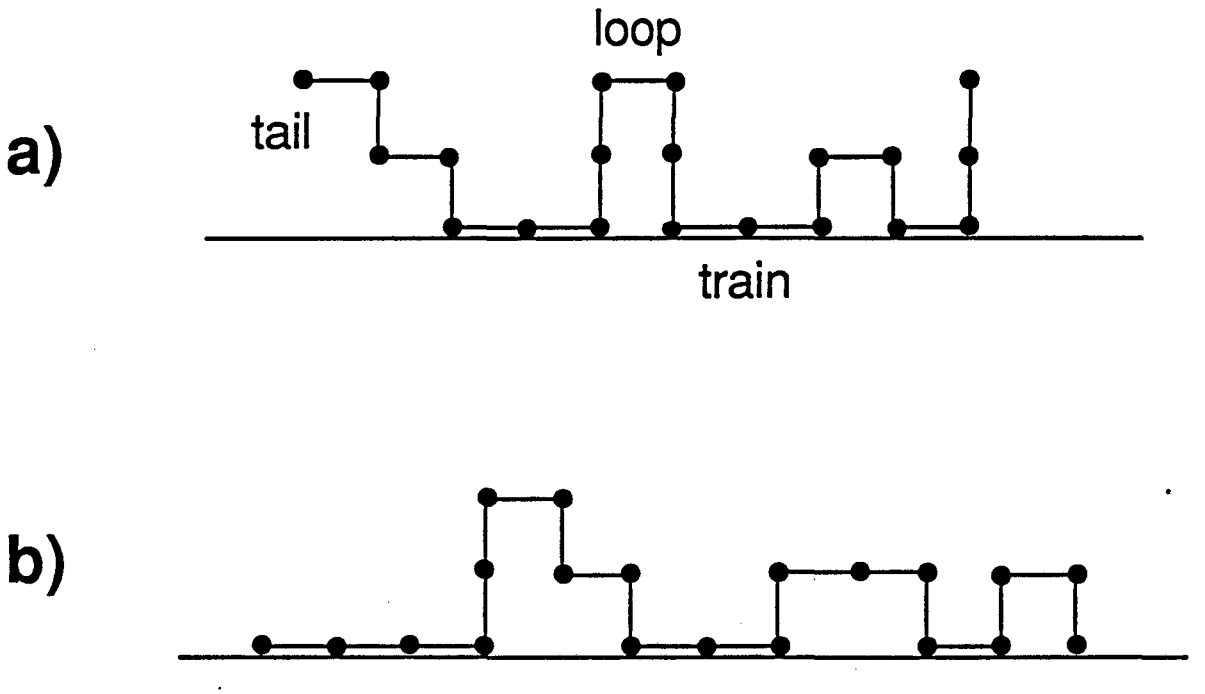

Figure 1

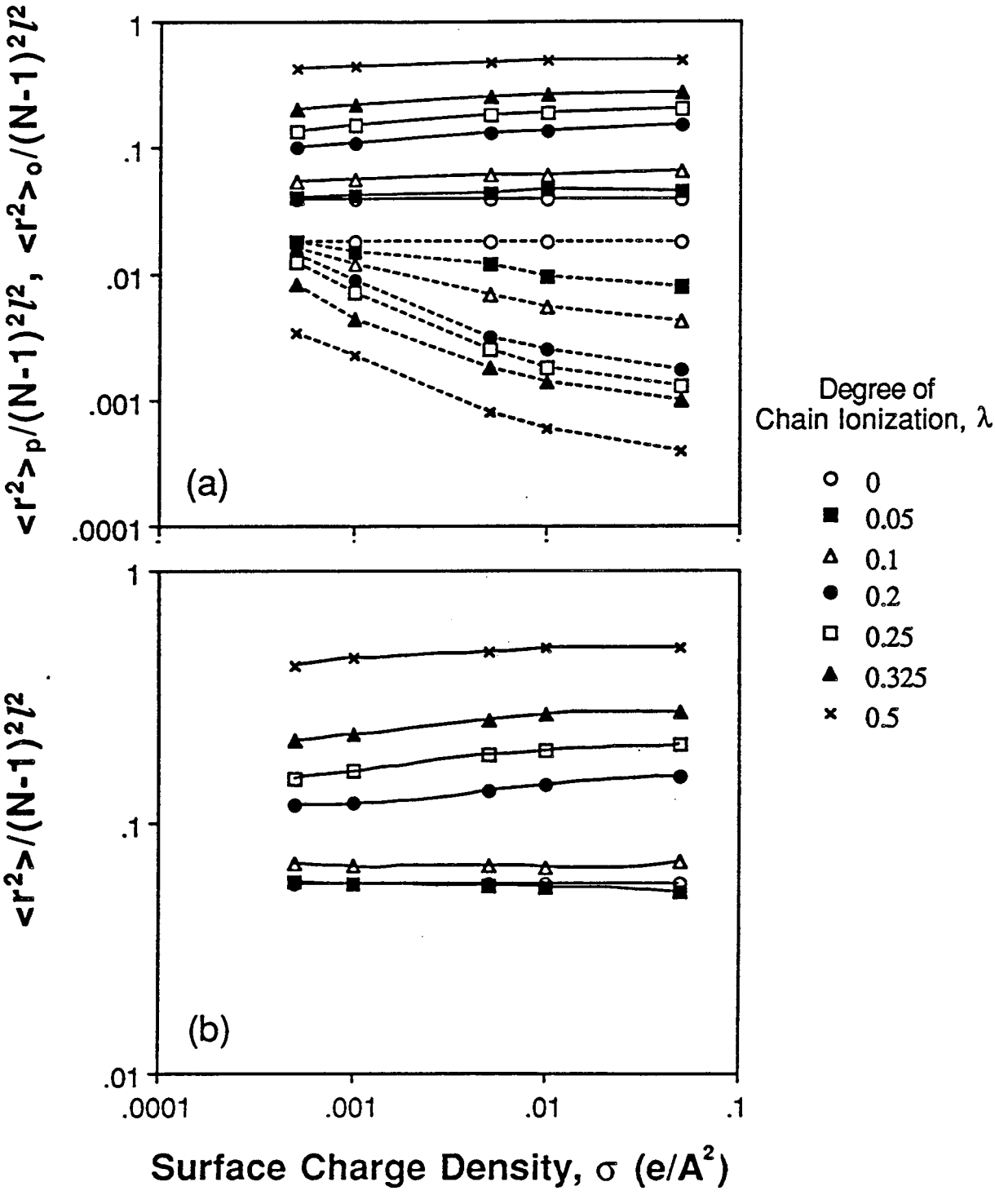
$\langle r^2\rangle_p/(N-1)^2l^2$, $\langle r^2\rangle_o/(N-1)^2l^2$
1
.1
.01
.001
.0001
(a)
$\langle r^2\rangle/(N-1)^2l^2$
1
.1
.01
(b)
.0001
.001
.01
.1
Surface Charge Density, σ (e/A²)
Degree of Chain Ionization, λ
0
0.05
0.1
0.2
0.25
0.325
0.5

Figure 2

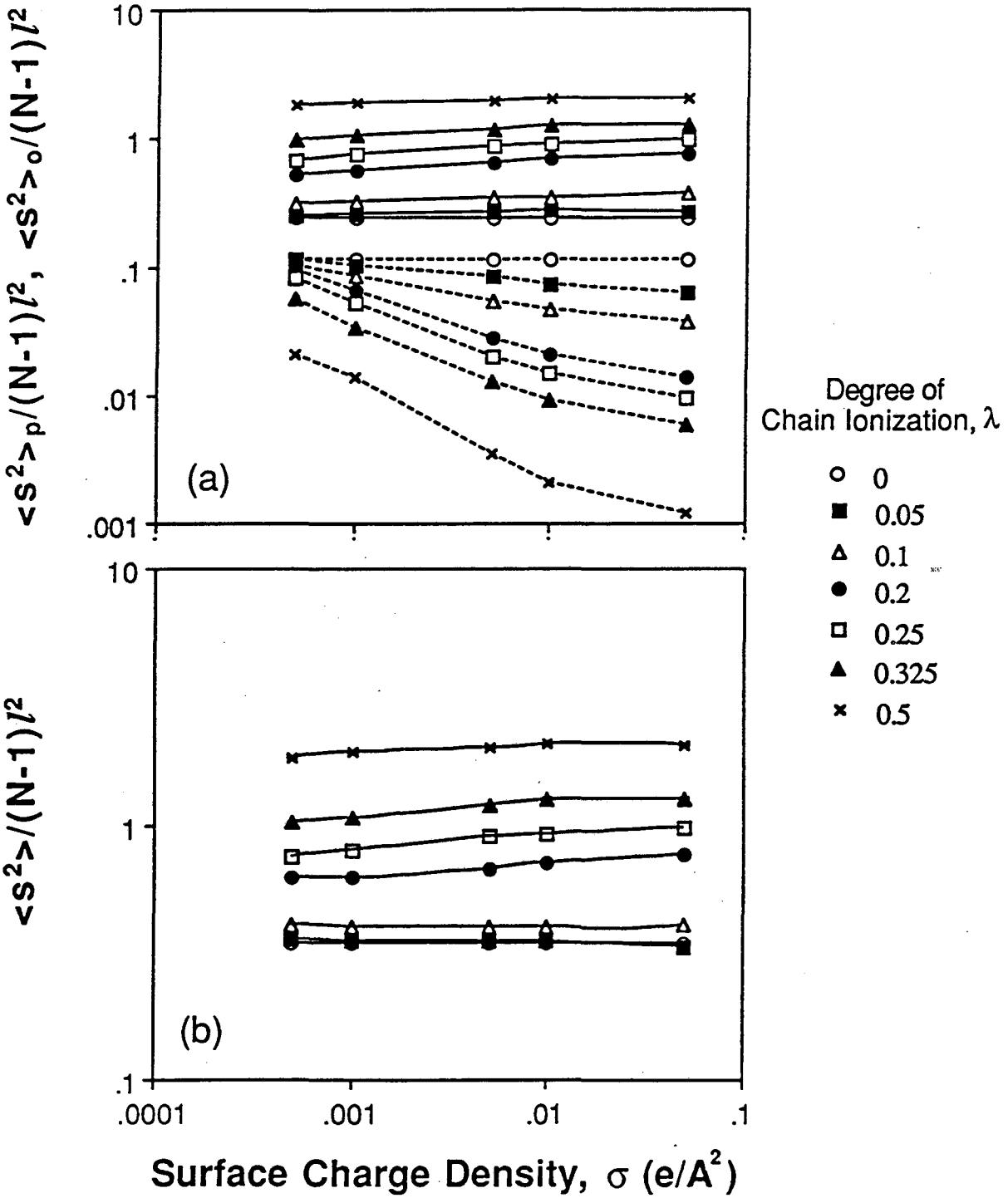
10
1
.1
.01
.001
(a)
$<s^2>_p/(N-1)l^2$, $<s^2>_o/(N-1)l^2$
10
1
.1
(b)
$<s^2>/(N-1)l^2$
.0001
.001
.01
.1
Surface Charge Density, σ (e/A²)
Degree of Chain Ionization, λ
0
0.05
0.1
0.2
0.25
0.325
0.5

Figure 3

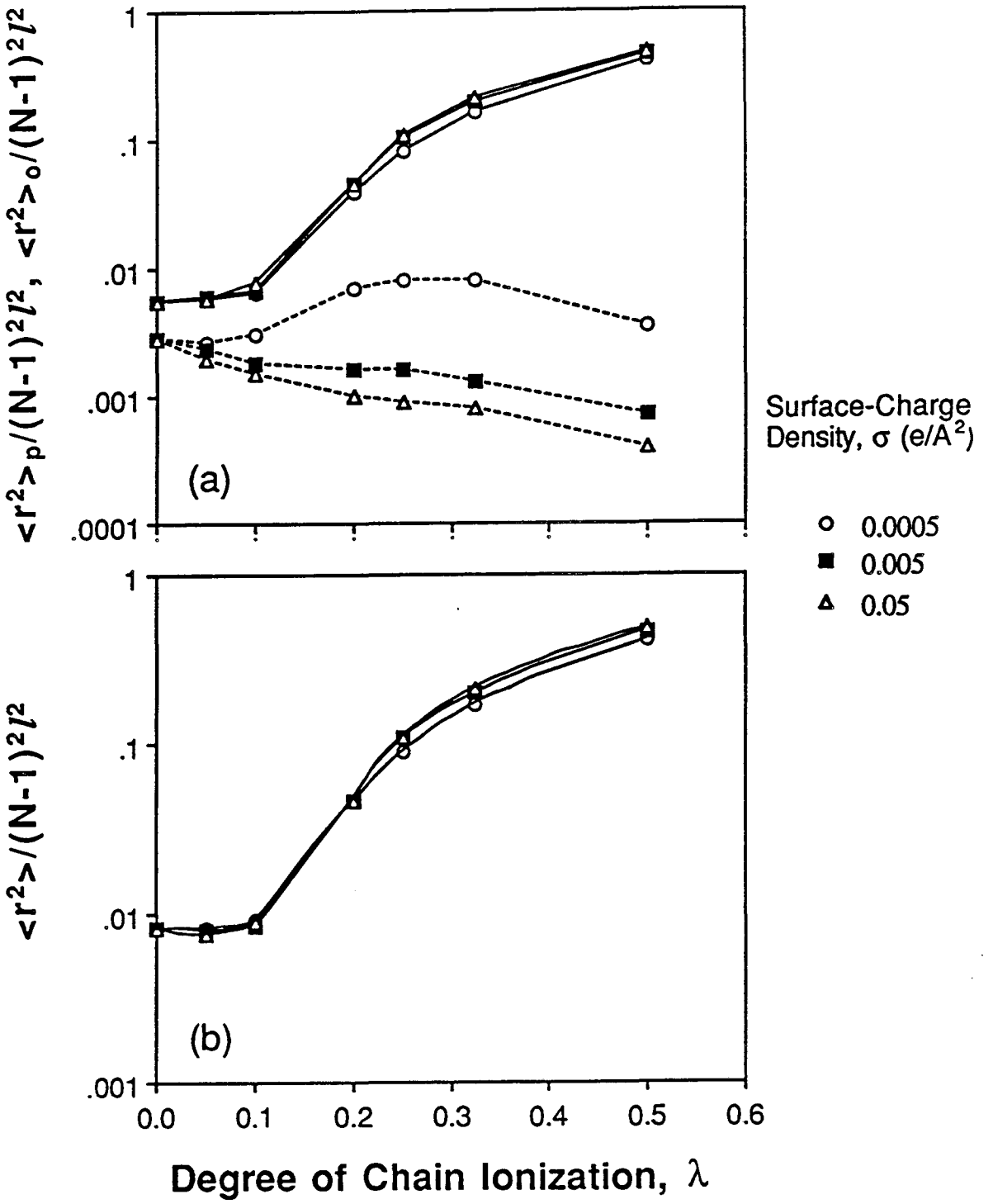
$\langle r^2\rangle_p/(N-1)^2l^2$, $\langle r^2\rangle_o/(N-1)^2l^2$
1
.1
.01
.001
.0001
(a)
Surface-Charge Density, σ (e/A²)
0.0005
0.005
0.05
$\langle r^2\rangle/(N-1)^2l^2$
1
.1
.01
.001
(b)
0.0
0.1
0.2
0.3
0.4
0.5
0.6
Degree of Chain Ionization, λ

Figure 4

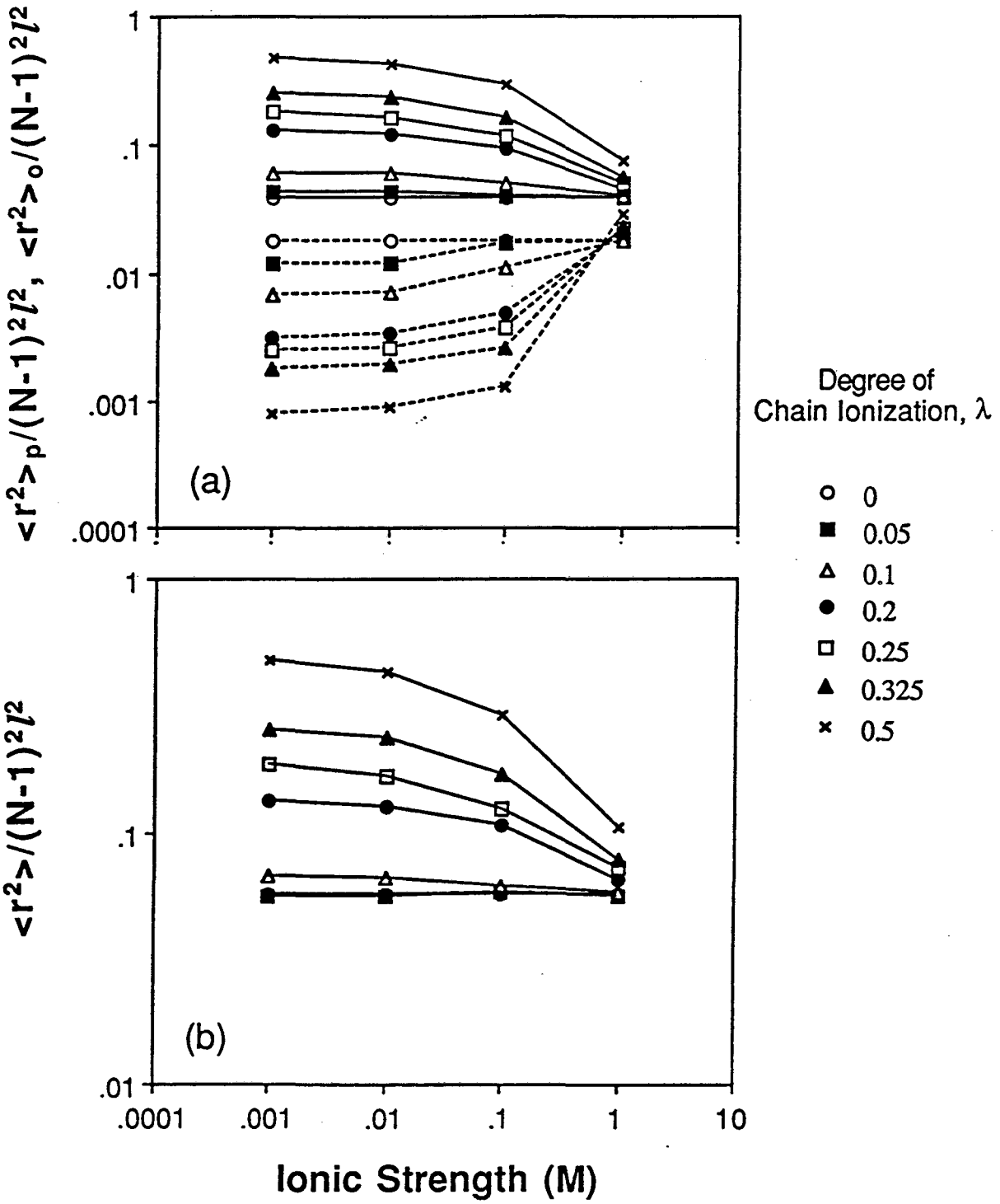
$\langle r^2\rangle_p/(N-1)^2l^2$, $\langle r^2\rangle_o/(N-1)^2l^2$
1
.1
.01
.001
.0001
(a)
$\langle r^2\rangle/(N-1)^2l^2$
1
.1
.01
(b)
.0001
.001
.01
.1
1
10
Ionic Strength (M)
Degree of Chain Ionization, λ
0
0.05
0.1
0.2
0.25
0.325
0.5

Figure 5

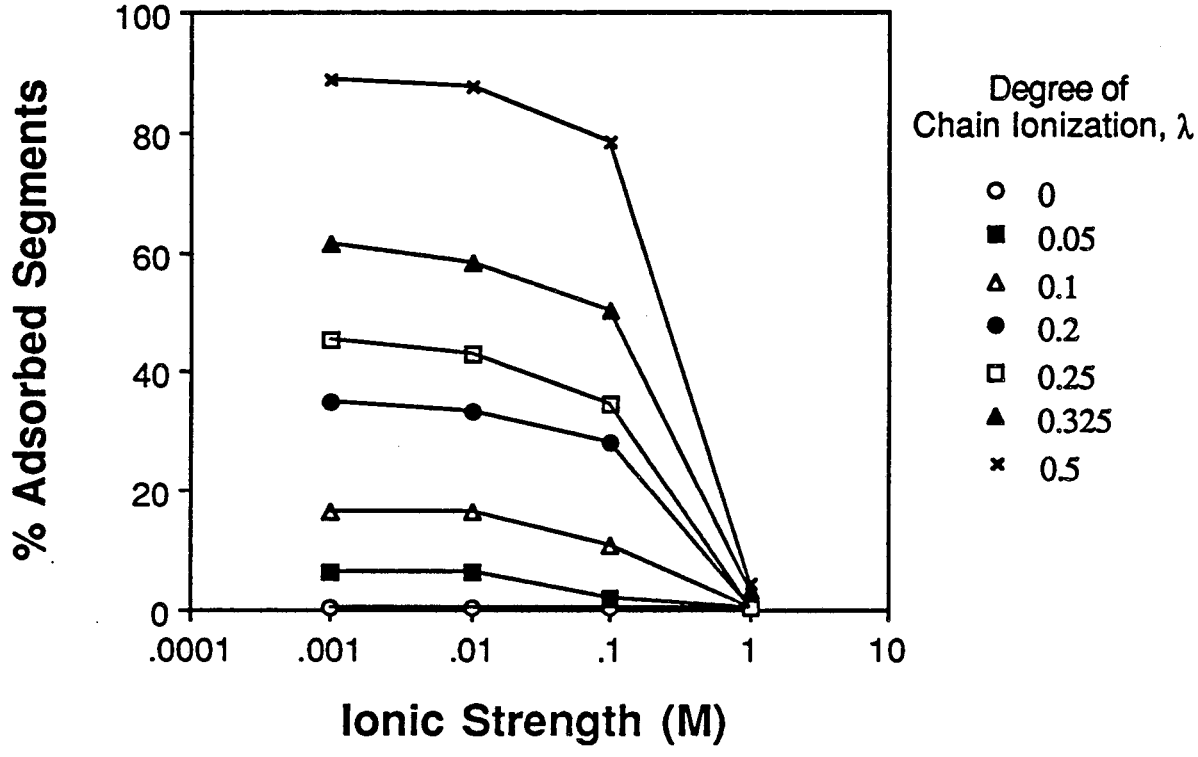
100
80
60
40
20
0
% Adsorbed Segments
.0001
.001
.01
.1
1
10
Ionic Strength (M)
Degree of
Chain Ionization, λ
0
0.05
0.1
0.2
0.25
0.325
0.5

Figure 6

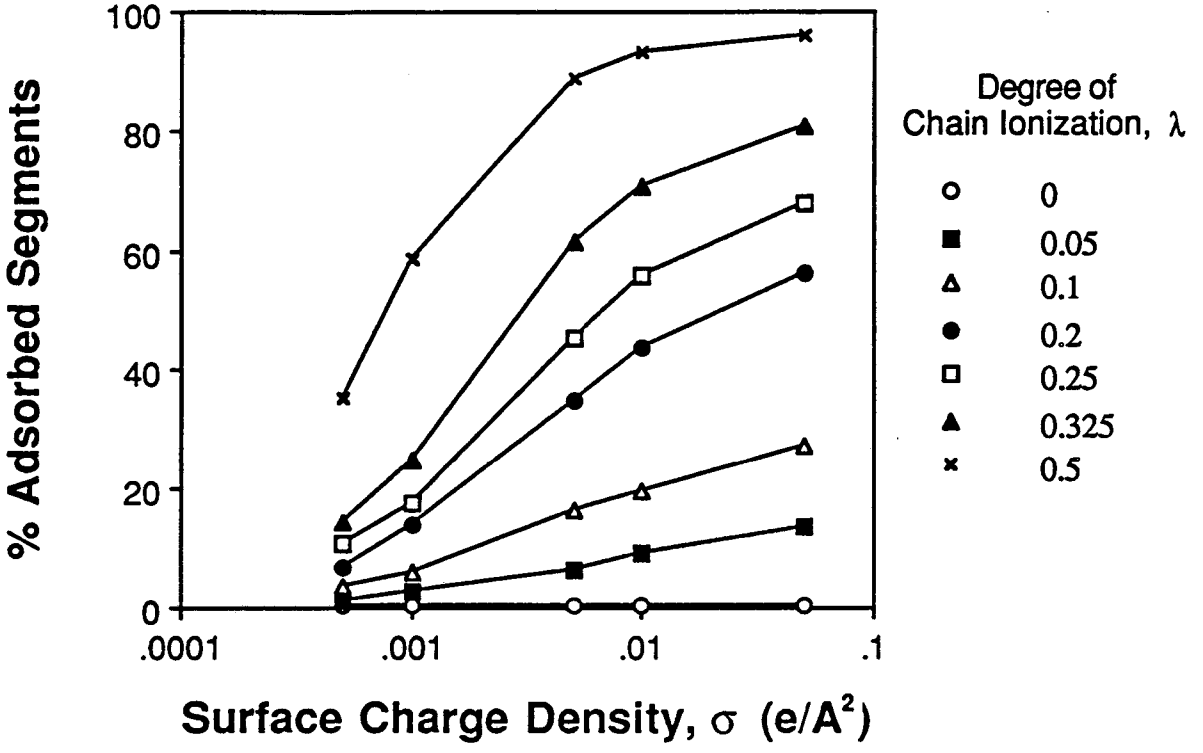
100
80
60
40
20
0
% Adsorbed Segments
.0001
.001
.01
.1
Surface Charge Density, σ (e/A²)
Degree of
Chain Ionization, λ
0
0.05
0.1
0.2
0.25
0.325
0.5

Figure 7

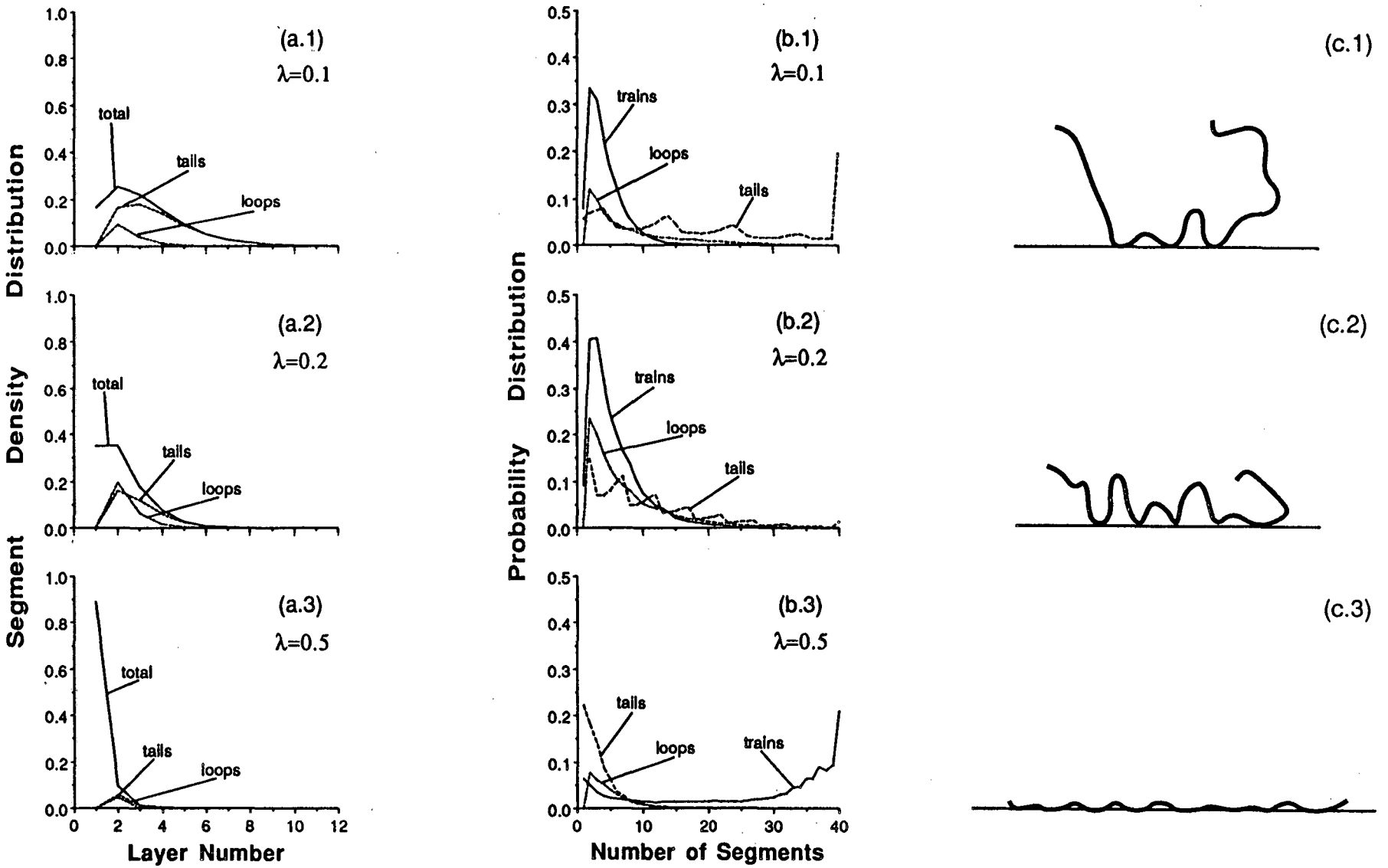
(a.1)
λ=0.1
total
tails
loops
(a.2)
λ=0.2
total
tails
loops
(a.3)
λ=0.5
total
tails
loops
Segment Density Distribution
Layer Number
(b.1)
λ=0.1
trains
loops
tails
(b.2)
λ=0.2
trains
loops
tails
(b.3)
λ=0.5
tails
loops
trains
Probability Distribution
Number of Segments
(c.1)
(c.2)
(c.3)

Figure 8

LAWRENCE BERKELEY LABORATORY
UNIVERSITY OF CALIFORNIA
INFORMATION RESOURCES DEPARTMENT
BERKELEY, CALIFORNIA 94720